JOURNAL OF MATERIALS SCIENCE 27 (1992) 1332–1336

Preparation of micaceous iron oxide by the oxidation of iron with pressurized oxygen in concentrated sodium hydroxide solution at elevated temperatures

S. UCHIDA, T. SATO, A. OKUWAKI
Department of Molecular Chemistry and Engineering, Tohoku University, Sendai 980, Japan

Iron powders were oxidized in NaOH solutions of 5–25 mol kg^{-1} at 403–563 K and 5 MPa of oxygen partial pressure. Various types and morphologies of iron compounds such as fine particles of Fe_3O_4, micaceous α-Fe_2O_3, and coagulated particles of α-$NaFeO_2$ were formed depending on the experimental conditions. The observed critical concentrations of NaOH above which α-$NaFeO_2$ was formed was in good agreement with those thermodynamically calculated for the hydrolysis equilibrium of α-$NaFeO_2$.

1. Introduction

Recently fabrication of ceramic materials by the hydrothermal oxidation of metals and alloys has received special attention because of advantages such as high purity and excellent morphology of products, high reaction rate, etc. Many studies have been carried out on the oxidation of iron under the hydrothermal conditions, since it is useful to synthesize fine particles of magnetic iron oxide, Fe_3O_4, and is also important in clarifying the corrosion behaviour of steels [1–5]. It is well known that various kinds of iron compounds such as FeOOH, Fe_3O_4, α-Fe_2O_3, γ-Fe_2O_3, Na_4FeO_4, Na_2FeO_4 [3], etc. may be formed by the oxidation of iron in aqueous solutions. The crystalline phases and morphologies of iron compounds depend significantly on the reaction conditions such as temperature, pH, coexisting ion, etc. For example spherical [6], cubic [7, 8], spindle-type [9], doubly spherical [10] and disc-like [11] α-Fe_2O_3 were fabricated by the forced hydrolysis of iron salts solutions at elevated temperatures. It was also reported that micaceous iron oxide, α-Fe_2O_3 which has received attention for protective coating applications could be obtained by the oxidation of Fe^{2+} ion in concentrated alkaline solutions at elevated temperatures [12, 13]. Hydrothermal oxidation of iron seemed to be desirable for the fabrication of iron oxides because of the lack of alkali consumption for neutralization. However, it is difficult to grow a desired compound as single phase, e.g. although α-Fe_2O_3 should be the stable phase in Fe–H_2O system up to about 1050 °C, Fe_3O_4 can sometimes form at moderate temperatures. Further, there are few fundamental data concerning the formation diagram for the hydrothermal oxidation of iron [14]. In the present study, iron powder was oxidized in concentrated NaOH solutions at elevated temperatures under pressurized oxygen and the formation diagram of various iron compounds was constructed where hydrolysis of α-$NaFeO_2$ to α-Fe_2O_3 was also discussed.

2. Experimental procedure

The reagent grade reduced iron powder of mean particle size of about 100 µm, was used as a starting material. The chemical analysis of the iron powder reported by the supplier was as follows: water soluble matter < 0.15%, sulphuric acid insoluble matter < 1.0%, S < 0.02%, As < 0.0015%. Sodium hydroxide was of reagent grade and was used without further purification.

Water was obtained through an ion exchanger from distilled water. Hydrothermal oxidation of iron powders was conducted in an autoclave of 300 cm^3 internal volume with a magnet driving stirrer fabricated from SUS 316 type stainless steel. Polytetrafluoroethylene (Teflon®) cup inserts of 2 mm wall thickness were used in the reaction vessel. The stirring rod and blade were coated with Teflon® tape to avoid corrosion.

A typical experiment proceeded as follows: three grams of reduced iron powder, 50 g of water and 10–50 g of sodium hydroxide were placed into a Teflon cup contained in an autoclave, and then the autoclave was sealed. After the removal of air by replacing with nitrogen gas, the autoclave was placed in an electric furnace, and the temperature was raised at a heating rate of about 6 °C min^{-1} to a desired temperature under saturated vapour pressure, followed by injecting oxygen gas into the autoclave up to 5 MPa of the oxygen partial pressure to start the oxidation reaction. During the reaction period, the suspensions were agitated at the rate of 1200 r.p.m. and the oxygen partial pressure was kept at 5 MPa. After maintaining at the desired temperature for 2 h, the autoclave was removed from the electric furnace,

0022-2461

cooled quickly in air, and the reaction products taken out and separated centrifugally, rinsed with methanol and dried at 105 °C for 12 h. The crystalline phases of the products were determined by X-ray powder diffraction analysis (XRD) using Fe filtered CoK_α radiation. The microstructures of the samples were observed by scanning electron microscopy (SEM). The amount of hydrogen was determined by gas chromatography.

3. Results and discussion

Iron powders were oxidized in 5–25 mol(kg $H_2O)^{-1}$ NaOH solutions at 403–563 K in the presence and absence of 5 MPa of O_2 for 2 h. Although only small crystals of Fe_3O_4 with octahedral symmetry were formed by the hydrothermal oxidation of iron in the absence of oxygen as previously reported [15], various kinds of iron compounds were obtained under pressurized oxygen. X-ray powder diffraction profiles and scanning electron micrographs of the samples obtained under various reaction conditions in the presence of oxygen are shown in Figs 1 and 2. Samples (a)–(d) were fabricated in NaOH solutions of 5, 15, 10 and 25 mol(kg $H_2O)^{-1}$ at 403, 483, 523 and 523 K, respectively, at 5 MPa of the oxygen partial pressure for 2 h. The X-ray powder diffraction profiles of samples a–d could be attributed to the mixture of α-Fe and α-Fe_2O_3, Fe_3O_4, α-Fe_2O_3 and α-$NaFeO_2$, respectively, and could be indexed as shown in Fig. 1. Sample a consisted of coagulated iron particles of mean diameter of 100 μm. Although sample a showed strong XRD peaks corresponding to (1 1 0) of α-Fe together with small XRD peaks corresponding to α-Fe_2O_3, the microstructures of the sample a were almost the same as those of the original iron particles. Therefore, it may be concluded that the hydrothermal oxidation of iron is slow at 403 K. Sample b, Fe_3O_4, consisted of blackish fine particles, 0.5–1.0 μm in diameter, with octahedral symmetry. On the other hand, sample c, α-Fe_2O_3, consisted of large hexagonal plate-like micaceous particles, ≃ 30 μm in diameter and 2 μm in thickness. Although α-Fe_2O_3, with smaller crystals is red-brown, sample c was metallic greyish silver. Since the XRD peak intensity ratio, I/I_0 of (0 0 6) plane of present micaceous α-Fe_2O_3 was 3.2 times stronger than that in JCPDS card 33-664, the plate-like plane might be {0 0 1}. Sample d, α-$NaFeO_2$, was reddish-black and consisted of large particles, ca. 30 μm in diameter, formed by coagulation of fine particles of 2–5 μm in diameter.

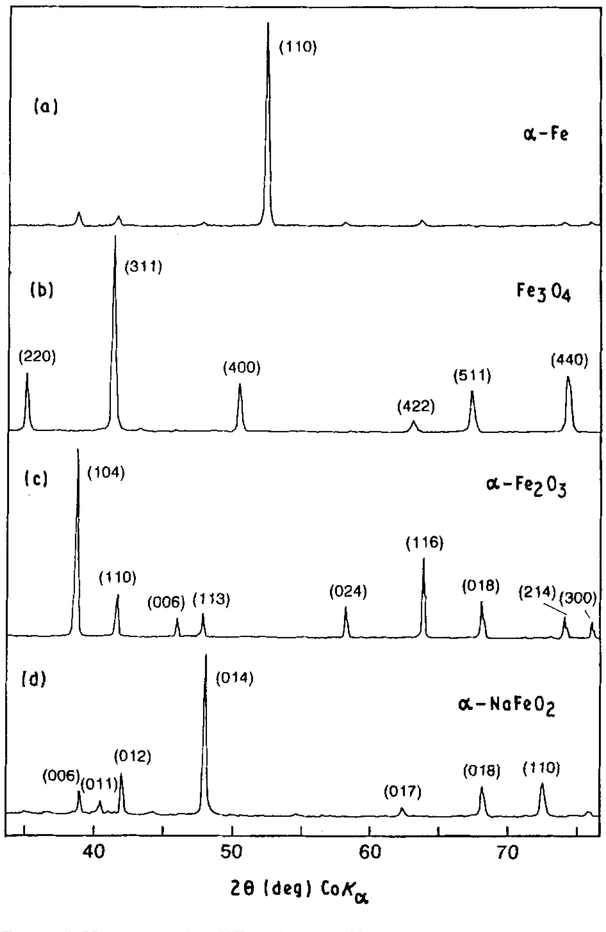

Figure 1 X-ray powder diffraction profiles of the samples produced by the oxidation of iron powder in sodium hydroxide solutions at elevated temperatures and 5 MPa of oxygen partial pressure for 2 h. NaOH concentrations and temperatures for samples (a), (b), (c) and (d) are 5, 15, 10 and 25 mol(kg $H_2O)^{-1}$ and 403, 483, 523 and 523 K, respectively.

The crystalline phases of the samples formed under various NaOH concentrations and temperatures at 5 MPa of the oxygen partial pressure are summarized in Fig. 3. It is seen that the hydrothermal oxidation of iron hardly proceeded at temperatures lower than 403 K and/or NaOH concentrations lower than 5 mol(kg $H_2O)^{-1}$. Magnetite was usually formed as mixtures with α-Fe_2O_3 or α-$NaFeO_2$ in 10–20 mol (kg $H_2O)^{-1}$NaOH solutions at 443–483 K. It is notable that large micaceous iron oxide, α-Fe_2O_3, could be fabricated as single phase above 473 K in 5–10 mol(kg $H_2O)^{-1}$NaOH solutions. It was notable to remember that only Fe_3O_4 was formed in the absence of oxygen. Magnetite formed in the absence of oxygen could not be converted to α-Fe_2O_3 under the present experimental conditions even though oxygen gas was supplied. Significant amounts of hydrogen were detected in the gas phases by gas chromatography whenever Fe_3O_4, α-Fe_2O_3 and α-$NaFeO_2$ were formed. According to the present experimental results and the knowledge [3] that divalent iron is soluble in concentrated NaOH solution as ferrate(II), FeO_2^{2-}, it can be speculated that the first stage of the reaction of the hydrothermal oxidation of iron is the formation of ferrate(II) and hydrogen as expressed by Equation 1.

$$\mathrm{Fe(s) + 2NaOH(aq) = Na_2FeO_2(aq) + H_2(g)} \tag{1}$$

Then, Fe_3O_4 and α-Fe_2O_3 might be formed competitively by the overall reactions expressed by Equations 2 and 3.

$$\begin{aligned}\mathrm{3Na_2FeO_2(aq) + 4H_2O(l)} &= \mathrm{Fe_3O_4(s)} \\ &\quad \mathrm{+ 6NaOH(aq) + H_2(g)}\end{aligned} \tag{2}$$

$$\begin{aligned}\mathrm{2Na_2FeO_2(aq) + \tfrac{1}{2}O_2(g) + 2H_2O(l)} \\ \mathrm{= Fe_2O_3(s) + 4NaOH(aq)}\end{aligned} \tag{3}$$

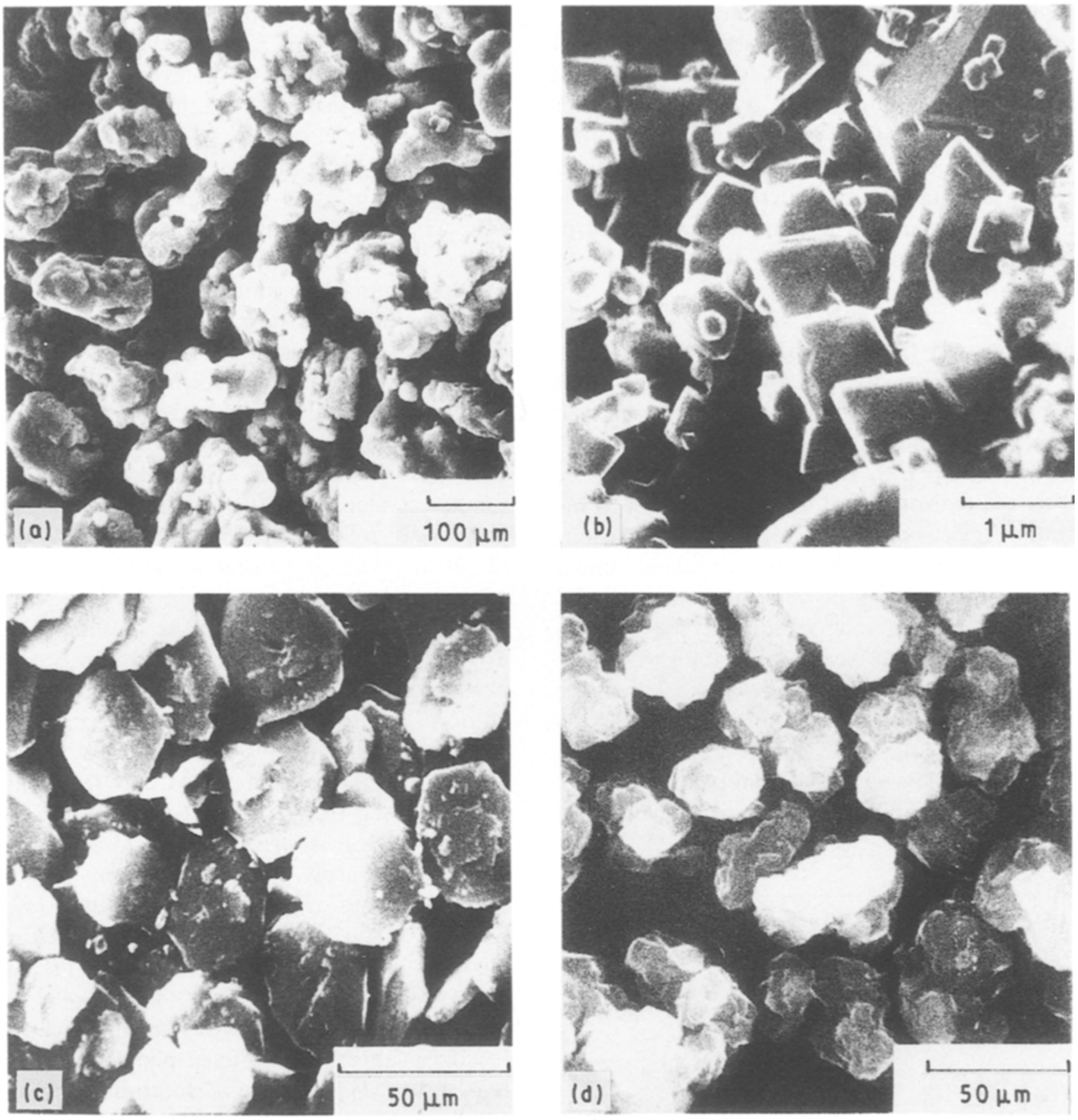

Figure 2 Scanning electron micrographs of the samples produced by the oxidation of iron powder in sodium hydroxide solutions at elevated temperatures and 5 MPa of oxygen partial pressure for 2 h. NaOH concentrations and temperatures for samples (a), (b), (c) and (d) are 5, 15, 10 and 25 mol $(\text{kg}\,H_2O)^{-1}$ and 403, 483, 523 and 523 K, respectively.

Since Fe_3O_4 is not thermodynamically stable under the present reaction conditions, it should exist as a meta-stable phase. Although the formation of Fe_2O_3 by the hydrothermal reaction expressed by Equation 4 might also be thermodynamically possible, it hardly seemed to proceed under the present experimental conditions, because only Fe_3O_4 was detected in the absence of oxygen.

$$2Na_2FeO_2(aq) + 4H_2O(l) = Fe_2O_3(s) + H_2(g) + 4NaOH \quad (4)$$

On the other hand, the hydrolysis of α-$NaFeO_2$ might be expressed by Equation 5.

$$Fe_2O_3(s) + 2NaOH(aq) = 2NaFeO_2(s) + H_2O(l) \quad (5)$$

This reaction determines the NaOH concentration controlling the stability relations of α-Fe_2O_3 and α-$NaFeO_2$ in 10–25 mol $(\text{kg}\,H_2O)^{-1}$. The NaOH concentration was calculated as follows. The standard free energy change, ΔG°_T, and the equilibrium constant, K_T for Equation 5 at temperature, T, can be expressed in terms of Equations 6 and 7.

$$\begin{aligned}\Delta G^\circ_T &= \Delta G^\circ_{298} - \Delta T \Delta S^\circ_{298} \\ &\quad + \int_{298}^{T} \Delta C^\circ_p \mathrm{d}T - T\int_{298}^{T} (\Delta C^\circ_p/T)\mathrm{d}T \\ \Delta T &= T - 298 \qquad (6) \\ \log K_T &= -\Delta G^\circ_T/2.303\mathrm{R}T \qquad (7)\end{aligned}$$

where ΔS°_{298} is the standard entropy change. Heat capacity C°_p can be calculated by Equation 8 as a function of temperature.

$$C^\circ_p = a + bT + cT^{-2} \quad (8)$$

The free energy changes and equilibrium constants for Equation 5 calculated at various temperatures and the thermodynamic data used for the calculation of them are tabulated in Tables I and II, respectively.

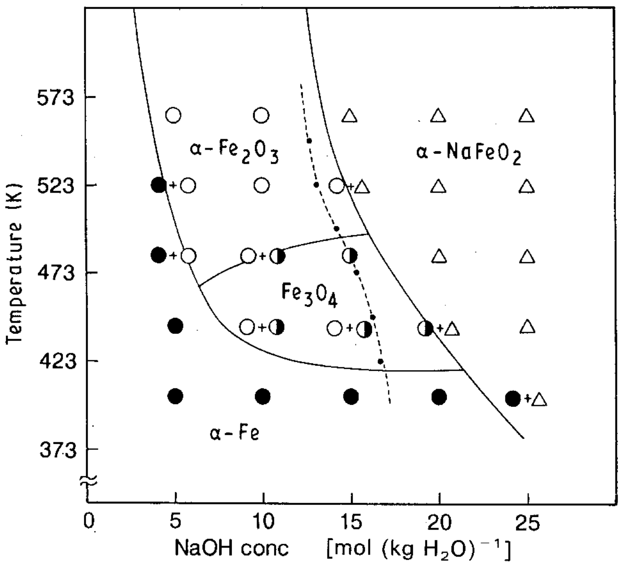

Figure 3 Crystalline phases of iron compounds formed by the oxidation of iron powder in sodium hydroxide solutions at elevated temperatures and 5 MPa of oxygen partial pressure for 2 h: (●) α-Fe; (◑) Fe_3O_4; (○) α-Fe_2O_3; (△) α-$NaFeO_2$, dotted line is the critical NaOH concentrations calculated by Equation 9.

TABLE I Standard free energy changes and equilibrium constants for Equation 5 at various temperatures

T(K)	ΔG°_T (kJ mol^{-1})	log K
298	3.63	− 11.1
423	2.70	− 5.84
448	2.42	− 4.93
473	2.10	− 4.06
498	1.75	− 3.22
523	1.38	− 2.42
548	0.985	− 1.64

Since the equilibrium constant for Equation 5 can be expressed as a function of NaOH concentration as shown by Equation 9, the critical NaOH concentration above

$$K = a^2_{NaFeO_2} a_{H_2O} / a_{Fe_2O_3} a^2_{NaOH} = a_{H_2O}/a^2_{NaOH}$$
$$= a_{H_2O}/\gamma^2_{NaOH} m^2_{NaOH} = a_{H_2O}/\gamma^4_{\pm} m^4_{\pm} \qquad (9)$$

which $NaFeO_2$ is formed can be calculated, where a is activity, γ is the activity coefficient and m is molarity. The critical NaOH concentrations calculated at various temperatures are shown in Fig. 3 as a dotted line, where mean activity coefficients for NaOH, $\gamma_\pm$ and activity of water were estimated from the thermodynamic relation (Equation 11) and Pitzer's equations [21–23] expressed by Equation 10 and 12,

TABLE III Temperature dependence of the parameters in Pitzer's equation

T(K)	A_ϕ	$\beta^{(0)}$ (10^2)	$\beta^{(1)}$	C^ϕ (10^3)
298	0.390	8.80	0.253	3.96
423	0.526	6.51	0.504	− 0.477
448	0.567	5.88	0.551	− 0.695
473	0.615	5.50	0.589	− 0.946
498	0.673	5.30	0.610	− 1.21
523	0.745	5.19	0.608	− 1.43
548	0.839	5.08	0.578	− 1.56

$$\begin{aligned} \ln\gamma_\pm &= -A_\phi[m^{1/2}/(1 + bm^{1/2}) \\ &\quad + (2/b)\ln(1 + bm^{1/2})] + 2m\beta^{(0)} \\ &\quad + (2\beta^{(1)}/\alpha^2)[1 - (1 + \alpha m^{1/2} \\ &\quad - \alpha^2 m/2)\exp(-\alpha m^{1/2})] + 3m^2 C^\phi/2 \\ b &= \tfrac{1}{2}, \quad \alpha = 2 \qquad (10) \\ \ln a_{H_2O} &= -2\phi m_{NaOH} M_{H_2O}/1000 \qquad (11) \\ \phi - 1 &= -A_\phi m^{1/2}/(1 + bm^{1/2}) \\ &\quad + m[\beta^{(0)} + \beta^{(1)}\exp(-\alpha m^{1/2})] \\ &\quad + m^2 C^\phi \qquad (12) \end{aligned}$$

where M is molecular weight, ϕ is the osmotic coefficient, A_ϕ is Debye–Hückel's limiting slope for the osmotic coefficient and $\beta^{(0)}$, $\beta^{(1)}$, and C^ϕ are constants depending on the temperature and pressure. The values of A_ϕ, $\beta^{(0)}$, $\beta^{(1)}$ and C^ϕ used for the calculation of the activity coefficients of NaOH and water are tabled in Table III. As seen in Fig. 3, the critical concentrations of NaOH calculated were in good agreement with those observed above 473 K. Therefore, it might be concluded that the equilibrium of Equation 5 was attained within 2 h above 473 K.

Below 473 K, the difference in the critical NaOH concentrations between calculated and observed tends to increase. This may be caused by the slow rate of oxidation and the error in the calculation of activities of water and NaOH. Equations 10 and 12 can be applied for concentrations up to 10 mol kg^{-1} NaOH solution.

4. Conclusions

From the present results, following conclusions may be drawn.

1. Micaceous iron oxide (α-Fe_2O_3), fine particles of Fe_3O_4 with octahedral symmetry and coagulated

TABLE II Thermodynamic data used for the calculation

Compound	ΔG°_{298} (kJ mol^{-1})	S°_{298} (J mol^{-1} K^{-1})	C°_p (J mol^{-1} K^{-1})		
			a	b (10^3)	c (10^{-5})
$NaFeO_2$ (c)	− 639[a]	88.3[a]	101[d]	23.1	− 16.7
Fe_2O_3 (c)	− 742[b]	87.4[b]	127[d]	13.8	− 20.9
NaOH (aq)	− 419[a]	48.1[a]	− 102[a]		
H_2O (l)	− 237[c]	69.9[c]	64.5[e]	33.5	

[a] [16]; [b] [17]; [c] [18]; [d] calculated by Kubaschewski method [19]; [e] calculated by least-squares method [20].

large particles of α-$NaFeO_2$ were formed by the oxidation of iron powder in concentrated NaOH solutions at elevated temperatures under pressurized oxygen.

2. The hydrolysis equilibrium between α-$NaFeO_2$ and α-Fe_2O_3 was attained within 2 h above 473 K, under the present experimental conditions.

3. The observed critical concentrations of NaOH above which α-$NaFeO_2$ was formed was in good agreement with those thermodynamically calculated for the hydrolysis equilibrium of α-$NaFeO_2$.

References

1. D. M. DRAZIC and C. S. HAO, *Electrochim. Acta* **27** (1982) 1409.
2. V. S. MURALIDHARN and M. VEERASHANMUGAMANI, *J. Appl. Electrochem.* **15** (1985) 675.
3. F. BECK, R. KAUS and M. OBERST, *Electrochim. Acta* **30** (1986) 173.
4. J.-Y. ZOU and D-T. CHIN, *ibid.* **32** (1987) 1751.
5. *Idem., ibid.* **33** (1988) 477.
6. E. MATIJEVIĆ and P. SCHEINER, *J. Colloid Interface Sci.* **63** (1978) 509.
7. S. HAMADA and E. MATIJEVIĆ, *ibid.* **84** (1981) 274.
8. M. OZAKI, S. KRATOHVIL and E. MATIJEVIĆ, *J. Chem. Soc. Faraday Trans. I*, **78** (1982) 2147.
9. S. HAMADA and E. MATIJEVIĆ, *J. Colloid Interface Sci.* **102** (1984) 146.
10. S. HAMADA, S. NIIZEKI and Y. KUDO, *Bull. Chem. Soc. Jpn.* **59** (1986) 3443.
11. R. S. SAPIESZKO and E. MATIJEVIĆ, *J. Colloid Interface Sci.* **74** (1980) 405.
12. S. NOBUOKA, in "Studies on Wet Process Synthesis of Magnetic Iron Oxide and Related Compounds" (Rep. Gov. Ind. Res. Inst., Osaka 1969) No. 331.
13. E. V. CARTER, *J. Oil Colour Chem. Assoc.* **71** (1988) 132.
14. G. PICARD, D. OSTER and B. TREMILLON, *J. Chem. Res.* (August 1980) 250.
15. S. HIRANO, S. SOMIYA, *J. Cryst. Growth* **35** (1976) 273.
16. "Selected Values of Chemical Thermodynamic Properties", edited by D. D. Wagman, W. H. Evans, V. B. Parker, R. H. Schumm and R. L. Nuttall, US (Department of Commerce, National Bureau of Standards, Washington, 1981) pp. 23, 47.
17. *Idem.*, in "Selected Values of Chemical Thermodynamic Properties", edited by D. D. Wagman, W. H. Evans, V. B. Parker, I. Halow, S. M. Bailey and R. H. Schumm (US Department of Commerce, National Bureau of Standards, Washington, 1969) p. 74.
18. *Idem.*, in "Selected Values of Chemical Thermodynamic Properties", edited by D. D. Wagman, W. H. Evans, V. B. Parkar, I. Halow, S. M. Bailey and R. H. Schumm, (US Department of Commerce, National Bureau of Standards, Washington, 1968) p. 13.
19. "Metallurgical Thermochemistry", 5th Edn, edited by O. Kubaschewski and C. B. Alcock (Pergamon Press, New York, 1979) pp. 180–5.
20. "JANAF Thermochemical Tables", 3rd Edn, Part II, Cr–Zr, edited by M. W. Chase, Jr., C. A. Davies, J. R. Downey, Jr., D. J. Fruip, R. A. McDonald and A. N. Syverud (American Chemical Society and the American Institute of Physics for the National Bureau of Standards, Michigan, 1985) Vol. 14, p. 1273.
21. R. T. PABALAN and K. S. PITZER, *Geochim. Cosmochim Acta* **51** (1987) 829.
22. "Thermodynamics", 2nd Edn, edited by K. S. Pitzer and L. Brewer, (McGraw-Hill Book Company, 1961) pp. 404–18.
23. "JSME STEAM TABLES" (The Japan Society of Mechanical Engineers, 1980) pp. 10–14.

Received 7 January
and accepted 13 May 1991